International Journal of Fracture (2005) 133:247–276
DOI 10.1007/s10704-005-4043-3

Fatigue strength of steel and aluminium welded joints based on generalised stress intensity factors and local strain energy values

P. LIVIERI[1] and P. LAZZARIN[2,*]
[1] *Department of Engineering, University of Ferrara, Via Saragat 1, 44100 Ferrara, Italy*
[2] *Department of Management and Engineering, University of Padova, Stradella S.Nicola 3,36100 Vicenza, Italy*
[*] *Author for correspondence (E-mail: plazzarin@gest.unip.it)*

Received 26 November 2004; accepted in revised form 18 March 2005

Abstract. Weld bead geometry cannot, by its nature, be precisely defined. Parameters such as bead shape and toe radius vary from joint to joint even in well-controlled manufacturing operations. In the present paper the weld toe region is modelled as a sharp, zero radius, V-shaped notch and the intensity of asymptotic stress distributions obeying Williams' solution are quantified by means of the Notch Stress Intensity Factors (NSIFs). When the constancy of the angle included between weld flanks and main plates is assured and the angle is large enough to make mode II contribution non-singular, mode I NSIF can be directly used to summarise the fatigue strength of welded joints having very different geometry. By using a large amount of experimental data taken from the literature and related to a V-notch angle of 135°, two NSIF-based bands are reported for steel and aluminium welded joints under a nominal load ratio about equal to zero. A third band is reported for steel welded joints with failures originated from the weld roots, where the lack of penetration zone is treated as a crack-like notch and units for NSIFs are the same as conventional SIF used in LEFM. Afterwards, in order to overcome the problem related to the variability of the V-notch opening angle, the synthesis is made by simply using a scalar quantity, i.e. the mean value of the strain energy averaged in the structural volume surrounding the notch tips. This energy is given in closed form on the basis of the relevant NSIFs for modes I and II and the radius R_C of the averaging zone is carefully identified with reference to conventional arc welding processes. R_C for welded joints made of steel and aluminium considered here is 0.28 mm and 0.12 mm, respectively. Different values of R_C might characterise welded joints obtained from high-power processes, in particular from automated laser beam welding. The local-energy based criterion is applied to steel welded joints under prevailing mode I (with failures both at the weld root and toe) and to aluminium welded joints under mode I and mixed load modes (with mode II contribution prevailing on that ascribable to mode I). Surprising, the mean value of ΔW related to the two groups of welded materials was found practically coincident at 2 million cycles. More than 750 fatigue data have been considered in the analyses reported herein.

Key words: Elasticity, energy, fatigue strength, notch stress intensity factor, stress intensity factor, welded joints.

1. Introduction

Weld bead geometry cannot be precisely defined mainly because parameters such as bead shape and toe radius vary from joint to joint even in well-controlled manufacturing operations (Radaj, 1990; Taylor et al., 2002). The weld toe radius decreases with the local heat concentration of the welding process, i.e. it is extremely small for automated high-power processes, especially for laser beam welding. Since also conventional arc welding techniques result in small values of toe radius (Yakubovskii and Valteris, 1989), in the Notch Stress Intensity Factor (NSIF) approach the weld toe region is modelled as a sharp V-notch and local stress distributions in plane cases are given on the basis of the relevant mode I and mode II NSIFs. The NSIFs simply quantify the magnitude of asymptotic stress distribution obeying Williams' solution (Williams, 1952). When the opening angle at the weld toe is large enough to result in a non-singular contribution for stress components due to the sliding mode (as happens, for example, in non-load-carrying transverse fillet welds), the fatigue behaviour can be correlated only to mode I NSIF (Lazzarin and Tovo, 1998).

It is worth noting that, after Radaj (1990), a comparison among different steel welded joints can be performed on the basis of the relevant theoretical stress concentration factors, after having imposed a fictitious notch radius ρ_f=1.0 mm. This value is valid only if the real radius at the weld toes and roots is thought of as zero.

Fatigue damage is generally described as the nucleation and growth of cracks to final failure, although the differentiation of two stages is "qualitatively distinguishable but quantitatively ambiguous" (Jiang and Feng, 2004). Initially thought of as parameters suitable for predicting only the fatigue limit (Atzori, 1985) or the fatigue crack initiation phase (Boukharouba et al., 1995; Verreman and Nie, 1996), NSIFs were found capable of predicting also total fatigue life (Lazzarin and Tovo, 1998; Atzori et al., 1999a, b, 2002; Lazzarin and Livieri, 2001; Lazzarin et al., 2003, 2004). This happens when a large amount of life is consumed at short crack depth, within the zone governed by the V-notch singularity. No demarcation line being drawn between fatigue crack initiation and early propagation, both phases are thought of as strictly dependent on the stress distribution initially present on the uncracked component.

Experimental investigations on transverse non-load-carrying fillet welded joints carried out by Lassen (1990) demonstrated that for various welding procedures, up to 40% of fatigue life was spent to nucleate a crack having a length of just 0.1 mm. Recent tests by Singh et al. (2003a, b) on load-carrying fillet joints in AISI 304L showed that the number of cycles required for the crack to grow by 0.5 mm in excess of the original lack of penetration reached 70% of total life.

The NSIF approach overcomes some difficulties inherent in the fatigue life concept based on fracture mechanics and, in particular, the very complex problems related to short crack propagation life and the multiple crack interaction on different planes, influenced by loading parameters and statistical variations related to the irregularity of the toe profile (Verreman and Nie, 1996). The NSIF approach has another advantage: the scale effect is fully included in the NSIF values, since the local stress distributions depend on the absolute dimensions of the joints.

Figure 1 shows some series of welded joints already analysed by Lazzarin and Tovo (1998). Original data were taken from Maddox (1987) and Gurney (1991) (see Table 2, series St1-12). In those series the main plate thickness ranged from 6 mm to 100 mm and the variation of the transverse stiffeners was even more pronounced (from 3 mm to 220 mm). All fatigue failures originated from the weld toes and the mean value of the weld angle did not vary ($2\alpha = 135°$). Due to large variations in the geometrical parameters, the scatter of the experimental data was obviously very pronounced in terms of nominal stress range. Figure 1 shows that the scatter greatly decreases as soon as the mode I NSIF (ΔK_1^N) is used as a meaningful parameter for

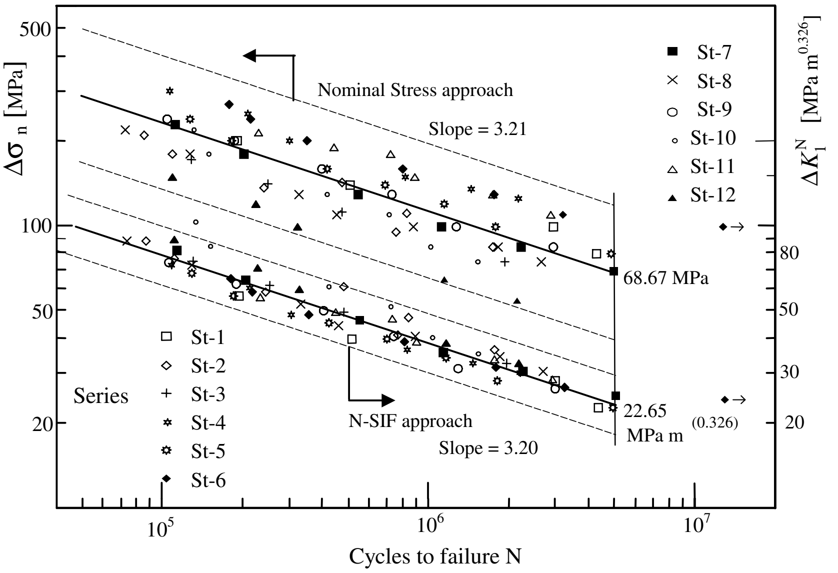

Figure 1. Fatigue data for as-welded joints in terms of nominal stress and NSIF ranges (after Lazzarin and Tovo, 1998). Original experimental data taken from Maddox (1987) and Gurney (1991), (see Table 2).

summarising fatigue total life data, without operating any distinction between fatigue crack nucleation and propagation.

From a theoretical point of view the NSIF-based band shown in Figure 1 cannot be applied to joints with a weld flank angle very different from 135°. That is simply because units for mode I NSIF are MPa(m)$^{\beta}$, where the exponent β depends on the V-notch angle, according to the expression $\beta = 1 - \lambda_1$, λ_1 being Williams' eigenvalue (Williams, 1952). This problem has been overcome in some recent papers by using the mean value of the strain energy density range (SER) present in a control volume of radius R_C surrounding the weld toe or the weld root (see Figure 2, Lazzarin and Zambardi, 2001, Lazzarin et al., 2003). The SER was given in closed form as a function of the relevant NSIFs, whereas R_C was thought of as dependent on welded material properties. The approach, reminiscent of Neuber "elementary volume" concept, was later applied to welded joints under multiaxial load conditions (Lazzarin et al., 2004). The simple volume shown in Figure 2 is not so different from that already drawn by Sheppard (1991) and Taylor (1999) while proposing a volume criterion based on local stresses to predict fatigue limits of notched components. Some analogies exist also with the highly stressed volume (the region where 90% of the maximum notch stress is exceeded) proposed by Sonsino dealing with high cycle strength of welded joints (Sonsino, 1995).

The aims of the present work are:

- To demonstrate that the scale effect exhibited by the welded joints depends on the V-notch angle. In the presence of fatigue failures nucleated from the weld root the exponent is expected to be about 0.5, so much greater than the value 0.25 suggested by Eurocode 3 (1993).
- To verify if a scatter band ΔW-N (strain energy range – number of cycles to failure) summarising about 300 fatigue data from welded joints with failures

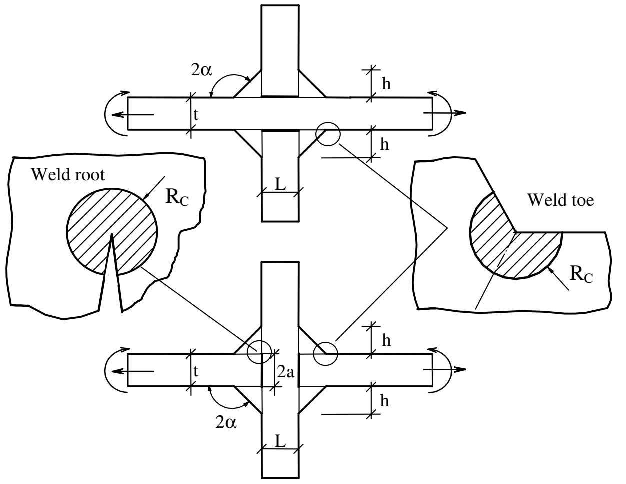

Figure 2. Geometrical parameters and critical volume (area) at the weld toes or roots.

systematically originated from the weld toes (Lazzarin et al., 2003) can be applied also to welded joints with failures from the weld roots. The joints considered here are transverse load-carrying fillet welded joints, made of ferritic steels BS 15, SM 41 e HT 60, as well as high-strength steels Domex 550 and ASTM 517F. Five series of welded joints made of AISI 304L and one series of Duplex 2205 are also analysed, showing the influence of the parent material.

- To provide a new ΔW-N band for aluminium welded joints, able to summarize the fatigue behaviour both of joints under prevailing mode I with failures at the weld toe as well as joints under mixed load condition, with mode II prevailing on mode I and failures at the weld roots. The ultimate tensile strength σ_u of all aluminium series considered here ranges from 300 MPa to 400 MPa, the only exception being the alloy 5052-H32 with $\sigma_u = 210$ MPa.
- To show that, by involving different values of the radius R_C, welded joints made of steel and aluminium alloy present approximately the same value of SER in the high cycle fatigue regime. This result is coherent with a diagram recently provided by Gómez and Elices (2003, 2004) dealing with the static behaviour of V-notched samples made of very different materials.

2. Analytical preliminaries

The degree of the singularity of the stress fields due to re-entrant corners was established by Williams both for modes I and II loading (Williams, 1952). When the weld toe radius ρ is set to zero, NSIFs quantify the intensity of the asymptotic stress distributions in the close neighbourhood of the notch tip. By using a polar coordinate system (r, θ) having its origin located at the sharp notch tip, the NSIFs related to modes I and II stress distribution are (Gross and Mendelson, 1972)

$$K_1^N = \sqrt{2\pi} \lim_{r\to 0^+} r^{1-\lambda_1} \sigma_{\theta\theta}(r, \theta = 0), \tag{1}$$

$$K_2^N = \sqrt{2\pi} \lim_{r\to 0^+} r^{1-\lambda_2} \sigma_{r\theta}(r, \theta = 0), \tag{2}$$

where the stress components $\sigma_{\theta\theta}$ and $\sigma_{r\theta}$ have to be evaluated along the notch bisector ($\theta = 0$). By means of Equations (1) and (2), it is possible to present Williams' formulae for stress components as explicit functions of the NSIFs. Then, mode I stress distribution is (Lazzarin and Tovo, 1996)

$$\begin{Bmatrix} \sigma_\theta \\ \sigma_r \\ \tau_{r\theta} \end{Bmatrix}_{\rho=0} = \frac{1}{\sqrt{2\pi}} \frac{r^{\lambda_1 - 1} K_1^{\mathrm{N}}}{(1+\lambda_1) + \chi_1 (1-\lambda_1)} \left[\begin{Bmatrix} (1+\lambda_1)\cos(1-\lambda_1)\theta \\ (3-\lambda_1)\cos(1-\lambda_1)\theta \\ (1-\lambda_1)\sin(1-\lambda_1)\theta \end{Bmatrix} + \chi_1 (1-\lambda_1) \begin{Bmatrix} \cos(1+\lambda_1)\theta \\ -\cos(1+\lambda_1)\theta \\ \sin(1+\lambda_1)\theta \end{Bmatrix} \right]. \tag{3}$$

Mode II stress distribution is

$$\begin{Bmatrix} \sigma_\theta \\ \sigma_r \\ \tau_{r\theta} \end{Bmatrix}_{\rho=0} = \frac{1}{\sqrt{2\pi}} \frac{r^{\lambda_2 - 1} K_2^{\mathrm{N}}}{(1-\lambda_2) + \chi_2 (1+\lambda_2)} \left[\begin{Bmatrix} -(1+\lambda_2)\sin(1-\lambda_2)\theta \\ -(3-\lambda_2)\sin(1-\lambda_2)\theta \\ (1-\lambda_2)\cos(1-\lambda_2)\theta \end{Bmatrix} + \chi_2 (1+\lambda_2) \begin{Bmatrix} -\sin(1+\lambda_2)\theta \\ \sin(1+\lambda_2)\theta \\ \cos(1+\lambda_2)\theta \end{Bmatrix} \right]. \tag{4}$$

With reference to some typical V-notch angles, Table 1 gives the parameters λ and χ for modes I and II stress distributions.

In many cases of practical interest, the geometry of the welded joint makes it possible to identify a nominal stress and correlate NSIFs to it. Two convenient expressions of NSIFs for welded joints are (Dunn et al., 1997; Lazzarin and Tovo, 1998)

$$\Delta K_1^{\mathrm{N}} = k_1 \Delta\sigma_n t^{1-\lambda_1}, \quad \Delta K_2^{\mathrm{N}} = k_2 \Delta\sigma_n t^{1-\lambda_2}, \tag{5a–b}$$

where k_i are non-dimensional coefficients, analogous to the shape functions of cracked components, $\Delta\sigma_n$ is the range of the remotely applied stress and t is the main plate thickness of the joints. Equations (5a–b) make it evident that:

Table 1. Parameters as a function of the V-notch angle. Coefficients e_1 and e_2 for plane strain conditions and Poisson's ratio $\nu = 0.3$.

2αrad	Mode I			Mode II		
	λ_1	χ_1	e_1	λ_2	χ_2	e_2
0	0.500	1.000	0.133	0.500	1.000	0.340
$\pi/6$	0.501	1.071	0.147	0.598	0.921	0.274
$\pi/4$	0.505	1.166	0.150	0.660	0.814	0.244
$\pi/3$	0.512	1.312	0.151	0.731	0.658	0.217
$\pi/2$	0.544	1.841	0.145	0.909	0.219	0.168
$2\pi/3$	0.616	3.003	0.129	1.149	−0.314	0.128
$3\pi/4$	0.674	4.153	0.118	1.302	−0.569	0.111
$5\pi/6$	0.752	6.362	0.104	1.486	−0.787	0.096

(a) the scale effect is fully included in NSIF definition. Two components scaled in geometrical proportion and subjected to the same nominal stress present a different value of NSIFs. When both contributions are singular, there is no possibility of identifying a single penalty coefficient able to link two different geometries scaled in geometrical proportion.
(b) mode II contribution is no longer singular when the V-notch angle is greater than 102.6°, since the exponent $1-\lambda_2$ is negative (Williams, 1952).

Expressions for k_1 and k_2 have already been reported in the literature for transverse non-load-carrying fillet welded joints subjected to tension or bending loadings. These expressions are reported in Appendix A, where their range of applicability is also defined. In addition, Appendix B reports Frank and Fischer's equations (1979) for conventional stress intensity factors of transverse load-carrying fillet welded joints with failure from the weld root. Finally, Appendix C gives two new expressions of k_1 and k_2 for load-carrying fillet welded joints with failure from the weld toe. These expressions summarise the results of a number of *ad hoc* FE analyses carried out by the present authors.

In a plane problem all stress and strain components in the highly stressed region are correlated to mode I and mode II NSIFs. Under a plane strain hypothesis, the strain energy included in a semicircular sector shown in Figure 2 is (Lazzarin and Zambardi, 2001)

$$\Delta\overline{\mathrm{W}} = \frac{e_1}{E}\left[\frac{\Delta K_1^{\mathrm{N}}}{R_{\mathrm{C}}^{1-\lambda_1}}\right]^2 + \frac{e_2}{E}\left[\frac{\Delta K_2^{\mathrm{N}}}{R_{\mathrm{C}}^{1-\lambda_2}}\right]^2, \tag{6}$$

where R_{C} is the radius of the semicircular sector and e_1 and e_2 are two functions that depend on the opening angle 2α and the Poisson ratio ν (see Table 1). A rapid calculation, with $\nu = 0.3$, can be made by using the following expressions (Lazzarin and Zambardi, 2001):

$$e_1 = -5.373\times10^{-6}(2\alpha)^2 + 6.151\times10^{-4}(2\alpha) + 0.1330, \tag{7}$$

$$e_2 = 4.809\times10^{-6}(2\alpha)^2 - 2.346\times10^{-3}(2\alpha) + 0.3400, \tag{8}$$

where 2α is in degrees. The material parameter R_{C} can be estimated by using the fatigue strength $\Delta\sigma_{\mathrm{A}}$ of the butt ground welded joints (in order to quantify the influence of the welding process, in the absence of any stress concentration effect) and the NSIF-based fatigue strength of welded joints having a V-notch angle at the weld toe constant and large enough to ensure the non-singularity of mode II stress distributions.

A convenient expression is (Lazzarin and Zambardi, 2001)

$$R_{\mathrm{C}} = \left(\frac{\sqrt{2e_1}\,\Delta K_{1\mathrm{A}}^{\mathrm{N}}}{\Delta\sigma_{\mathrm{A}}}\right)^{\frac{1}{(1-\lambda_1)}}, \tag{9}$$

where both λ_1 and e_1 depend on the V-notch angle. Equation (9) will be applied in the next sections of the paper taking into account the experimental value $\Delta K_{1\mathrm{A}}^{\mathrm{N}}$ at 5 million cycles related to transverse non-load carrying fillet welded joints with $2\alpha =$ 135° at the weld toe.

The hypothesis of constancy of R_C under mixed mode loads had been validated by Lazzarin and Zambardi (2001) by using experimental data mainly provided by Seweryn et al. (1997) and Kihara and Yoshii (1991). Seweryn investigated mixed-mode fracture of polymethyl-metacrylate (PMMA) specimens with a double symmetric V-notch with an opening angle 2α ranging from 20° to 80°. By modifying the orientation ψ of the specimen axis with respect to the applied tensile force, specimens were loaded in combined tension and shear. At two limit conditions, the middle cross section of the specimens was loaded by pure tension (when $\psi = 0°$) and by pure shear ($\psi = 90°$). Kihara and Yoshii (1991) tested under fatigue loading two materials and five geometries of plane specimens with V-shaped notches. Three geometries were characterised by single side and double side notches with 2α equal to 90° and 120°. Two other geometries were cruciform weld-like geometries with 2α equal to 135° and 135°. Mode II stress distributions were absent in the former three geometries, non-singular in the weld-like geometries. All experimental data were plotted in terms of $\Delta\bar{W}_1$, together with the value of R_C for the two steels. (Lazzarin and Zambardi, 2001).

Afterwards, a constant value of R_C was used to summarise in a single scatter band about 300 fatigue data related to steel welded joints with a V-notch angle at the weld toe ranging from 110° to 150° (Lazzarin et al., 2003). The relevant series are listed in Tables 2 and 3, where all material and geometrical properties are reported in detail. As far as welding technology is concerned, different arc welding processes had been used.

Finally, it is worth noting that when the V-notch becomes a crack-like notch ($2\alpha = 0$, $\lambda_1 = 0.5$ and $e_1 = 0.133$), Equation (9) gives

$$R_C = \frac{0.85}{\pi}\left(\frac{\Delta K_{th}}{\Delta\sigma_A}\right)^2 = 0.85\, a_0 \tag{10}$$

so that Equation (10) establishes a bridging between the value of R_C and the well known material parameter a_0 (El Haddad et al., 1979). However, the coefficient 0.85 would be different if one had used different working hypotheses (plane stress conditions instead of plane strain conditions, for example, or deviatoric strain energy density instead of total strain energy density).

3. Fatigue strength in terms of NSIF

All experimental data considered in the present paper are reported in Tables 2–6 for welded joints made of steel and in Tables 7 and 8 for welded joints made of aluminium. The tables give information about bibliographical references, welded joint materials, geometries, failure position, and high cycle fatigue strength. Fatigue strength properties are expressed in terms of nominal stress, NSIF and strain energy ranges. The complete data-base contains 820 fatigue data. Only 350 data and about half of the series (from St-1 to St-30 for steel welded joints, see Tables 2 and 3, and from AL-1 to AL-11 for aluminium welded joints, Table 7) had already been partially re-analysed in some previous papers (Lazzarin and Tovo, 1998; Lazzarin and Livieri, 2001; Lazzarin et al., 2003).

Table 2. Geometrical and fatigue strength properties of steel welded joints with failures from the weld toes. All joints were "as-welded". (Nominal load ratio $R \approx 0$, V-notch angle $2\alpha \cong 135^\circ$, radius $R_C = 0.3$ mm, according to Lazzarin et al. (2003)).

Series	Refs.	Welded joint geometry	Load	Material	σ_u MPa	t mm	L/t	$2h/t$	k_1	$\Delta\sigma_{n,50\%}$ MPa	$\Delta K^N_{1,50\%}$ MPa(mm)$^{0.326}$	$\Delta\bar{W}_{50\%}$ MJ/m^3
										Mean values at $N = 5 \times 10^6$ cycles		
St-1	Maddox, 1987	C-NLC	T	BS 4360:50B	562	13	0.769	1.231	1.14	79.5	209.4	0.055
St-2	Maddox, 1987	C-NLC	T	BS 4360:50D	573	50	1.000	0.640	1.10	59.6	234.2	0.069
St-3	Maddox, 1987	C-NLC	T	BS 4360:50D	550	100	0.500	0.320	0.88	55.5	219.8	0.061
St-4	Gurney, 1991	C-NLC	T	BS 4360:50D	548[c]	13	0.231	0.769	0.97	91.7	204.8	0.053
St-5	Gurney, 1991	C-NLC	T	BS 4360:50D	548[c]	13	0.769	1.231	1.14	76.7	202.0	0.051
St-6	Gurney, 1991	C-NLC	T	BS 4360:50	545[c]	25	0.120	0.400	0.79	93.9	211.1	0.056
St-7	Gurney, 1991	C-NLC	T	BS 4360:50	545[c]	25	1.280	0.720	1.15	66.0	217.4	0.059
St-8	Gurney, 1991	C-NLC	T	BS 4360:50	545[c]	25	8.800	1.200	1.36	61.6	239.1	0.072
St-9	Gurney, 1991	C-NLC	T	BS 4360:50D	527[c]	38	0.342	0.421	0.87	68.7	196.3	0.048
St-10	Gurney, 1991	C-NLC	T	BS 4360:50D	527[c]	38	5.789	0.789	1.41	45.5	209.5	0.055
St-11	Gurney, 1991	C-NLC	T	BS 4360:50D	509	100	0.030	0.100	0.55	95.7	236.6	0.070
St-12	Gurney, 1991	C-NLC	T	BS 4360:50D	509	100	2.200	0.300	1.27	40.1	228.7	0.066
St-13	Gurney, 1991	C-NLC	B	BS 4360:50	545[c]	25	0.120	0.400	0.79	87.9	198.6	0.050
St-14	Gurney, 1991	C-NLC	B	BS 4360:50D	531	50	0.060	0.200	0.66	98.1	232.4	0.068
St-15	Gurney, 1991	C-NLC	B	BS 4360:50D	509	100	0.030	0.100	0.59[b]	94.5	248.1	0.077
St-16	Gurney, 1991	C-NLC	B	BS 4360:5D	509	100	0.130	0.160	0.68	75.1	230.6	0.067

St-17	Kihl and Sarkani, 1997	C-NLC	T	HSLA-80	≈800	6	1.000	0.750[a]	1.11	103.1	205.7	0.053
St-18	Kihl and Sarkani, 1997	C-NLC	T	HSLA-80	≈800	19	1.000	0.750[a]	1.11	77.8	226.0	0.064
St-19	Kihl and Sarkani, 1997	C-NLC	T	HSLA-80	≈700	25	1.000	0.750[a]	1.11	57.4	182.2	0.042
St-20	Kihl and Sarkani, 1997	C-NLC	T	HSLA-80	≈700	11	1.000	0.750[a]	1.11	107.4	261.0	0.086
St-21	Kihl and Sarkani, 1999	C-NLC	T	HSLA-80	≈700	11	1.000	0.750[a]	1.11	93.6	227.3	0.065
St-22	Gurney, 1997	C-NLC	T	Low C Steel	515	6	1.000	2.000	1.20	93.6	201.4	0.051
St-23	Gurney, 1997	T-NLC	B	Low C Steel	515	6	1.000	2.000	1.07[b]	111.3	213.5	0.057
St-24	Gurney, 1997	C-LC	T	Low C Steel	515	6	1.000	2.000	1.45[b]	98.6	255.8	0.082

σ_u – ultimate tensile strength.

Type of load: T – tension load; B – bending load.

Type of joint: C-NLC – cruciform joint with non-load carrying fillet weld; C-LC – cruciform joint with load-carrying fillet weld; T-NLC – T-joint with non-load carrying fillet weld.

[a]value estimated from a figure of the original paper.

[b]$k_1$has been determined by means of "*adhoc*" FE analyses. For all other series, k_1 has been determined by means Equations (A.1) and (A.3).

[c]Mean value from different plates having the same thickness.

Table 3. Geometrical and fatigue strength properties from transverse non-load-carrying fillet welded joints. Materials were controlled-rolled and accelerated-cooled steels used in North Sea offshore platform structures. Welded joints stress-relieved with failures originated from the weld toes. (Tension loads with a nominal stress range $\Delta\sigma = 150\,\mathrm{MPa}$ and an effective load ratio $R \approx 0.3$; radius $R_C = 0.3\,\mathrm{mm}$ according to Lazzarin et al. (2003)).

Series	Refs.	Geometry	V-notch angle 2α degrees	$\beta = 1 - \lambda_1$	σ_u MPa	t mm	L/t	k_1	Mean values $N/10^3$	ΔK_1^N MPa (mm)$^\beta$	$\Delta\bar{W}_{50\%}$ MJ/m^3
St-25	Engesvik and Lassen, 1988	C-NLC	150	0.248	370	32	1	1.47	664	521	0.250
St-26	Engesvik and Lassen, 1988	C-NLC	120	0.384	510	25	1	0.874	327	452	0.323
St-27	Lassen, 1990	C-NLC	145	0.277	500	25	1	1.39	953	508	0.267
St-28	Lassen, 1990	C-NLC	125	0.367	500	25	1	0.981	585	480	0.340
St-29	Lassen, 1990	C-NLC	125	0.367	500	25	1	0.981	456	480	0.340
St-30	Lassen, 1990	C-NLC	110	0.414	500	25	1	0.778	370	442	0.348

Type of joint: C-NLC – cruciform joint with non-load carrying fillet weld.

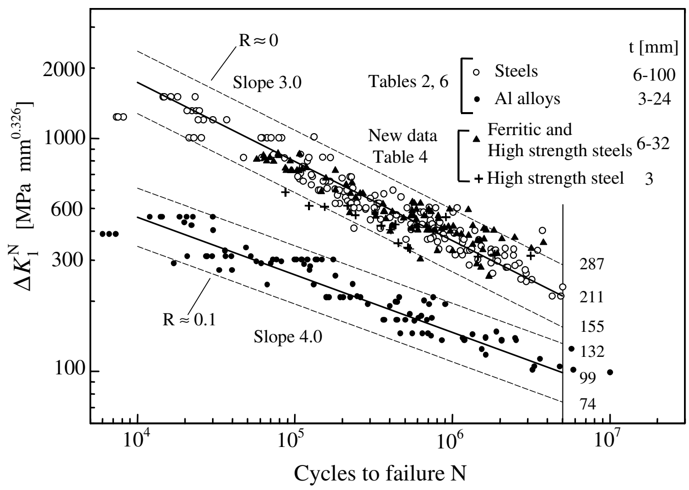

Figure 3. Fatigue strength of aluminium and steel welded joints as a function of mode I notch stress intensity factor. Scatter bands defined by mean values ±2 standard deviations.

Figure 3 shows the fatigue strength data related to steel and aluminium welded joints with a mean value of $2\alpha = 135°$ and all fatigue failures initiated at the weld toe. The new data, which concern ferritic steels BS 15 and SM 41 (ultimate tensile strength σ_u ranging from 420 MPa to 510 MPa) and the high strength steel Domex 550 (σ_u ranging from 600 MPa to 760 MPa, see Table 4), are plotted over a scatter band already reported in the literature (Lazzarin and Livieri, 2001). That band was based on the set of data of Table 2. The new data are found to be in satisfactory agreement with the old scatter band defined by mean values ± two standard deviations. The mean value of ΔK_1^N at 5×10^6 cycles ranges from 175 MPa to 247 MPa(mm)$^{0.326}$, showing a scatter analogous to that exhibited by the 24 series reported in Table 2, where the parameter ranged from 182 MPa to 261 MPa(mm)$^{0.326}$. It is worth noting that the maximum scatter concerned ferritic steel SM 41, series St-38 and St-41, and not the five series in Domex 550, which are fully included in the old scatter band. Figure 3 shows that the scatter index T_K related to two different probabilities of survival P_S (defined simply as $T_K = \Delta K_1^N{}_{,P_s=2.3\%} / \Delta K_1^N{}_{,P_s=97.7\%}$) is practically the same for steel and aluminium welded joints (1.80 against 1.85).

The curves and the scatter band of Figure 3 cannot be extended to load-carrying joints with crack initiation at the weld root. In these joints the V-notch angle, due to the lack of penetration, is $2\alpha = 0$ and units for NSIFs coincide with those of conventional SIF of linear elastic fracture mechanics. The material properties and geometrical parameters of the welded joints with failure from the weld root are summarised in Table 5. It is worth noting that in this type of joint both modes I and II stress distributions are singular close to the weld root. On the other hand, it is well known that the intensity of mode I distributions is much greater than that of mode II. Thus, only mode I NSIF values are reported in Table 5, all determined by using Frank and Fischer's equations (Frank and Fischer, 1979, see Appendix B).

The fatigue data are shown in Figure 4. The scatter band has been calculated by considering fatigue data from SM 41, BS 15, HT 60 and ASTM 517F steels, and then

Table 4. Geometrical and fatigue strength properties of steel welded joints with $2\alpha = 135^{\circ}$. All fatigue originated from the weld toes. (Nominal load ratio $R \approx 0$; radius $R_C = 0.28$ mm). Mean values at 5×10^6 cycles calculated by imposing a slope equal to 3.0 to all series.

Series	Refs.	Geometry	Load	Material	σ_u MPa	t mm	L/t	$2h/t$	a/t	k_1	$\Delta\sigma_{n,50\%}$ MPa	$\Delta K^{N}_{1,50\%}$ MPa (mm)$^{0.326}$	$\Delta\bar{W}_{50\%}$ MJ/m^3
											Mean values at $N = 5 \times 10^6$ cycles		
St-31	Gustafsson, 2002	C-NLC	T	Domex 550 MC	600–760	12	1	1.415	–	1.176	78	206	0.056
St-32	Gustafsson, 2002	C-NLC	B	Domex 550 MC	600–760	6	1	1.413	–	0.899	147	237	0.071
St-33	Gustafsson, 2002	C-NLC	B	Domex 550 MC	600–760	12	1	1.415	–	0.899	110	221	0.064
St-34	Gustafsson, 2002	C-NLC	T	Domex 550 MC	600–760	6	1	1.413	–	1.176	111	235	0.073
St-35	Gustafsson, 2002	C-NLC	T	Domex 550 MC	600–760	3	1	1.260	–	1.195	109	187	0.046
St-36	MacFarlane and Harrison, 1995	C-LC	T	BS 15	420	7.5	1	3.200	1	1.26	102	247	0.080
St-37	Kloppel and Weihermuller, 1959	C-LC	T	SM 41	510	14	1	2.000	1	1.39	75	247	0.080
St-38	Ouchida and Nishioka, 1966	C-LC	T	SM 41	450	16	1	1.750	0.125	0.979[a]	73	175	0.040
St-39	Ouchida and Nishioka, 1966	C-LC	T	SM 41	450	32	1	1.750	0.125	0.979[a]	65	196	0.051
St-40	Ouchida and Nishioka, 1966	C-LC	T	SM 41	450	16	1	0.875	0.125	1.16[a]	78	224	0.066
St-41	Ouchida and Nishioka, 1966	C-LC	T	SM 41	450	32	1	0.875	0.125	1.16[a]	67	241	0.073

σ_u – ultimate tensile strength.
Type of load: T – tension load; B – bending load.
Type of joint: C-NLC – cruciform joint with non-load carrying fillet weld; C-LC – cruciform joint with load-carrying fillet weld.
[a] k_1 determined by means of "*ad hoc*" finite element analyses. For the series 31–35, k_1 was determined by Equations (A.1) and (A.3), for the series 36–37 by Equation (C.1).

Table 5. Geometrical and fatigue strength properties of steel welded joints with $2\alpha = 0$ and failures from weld roots. (Nominal load ratio $R \approx 0$; radius $R_C = 0.28$ mm).

Series	Ref.	Geometry	Material	Load type	t mm	σ_u MPa	L/t	$2h/t$	$2a/t$	k_1^a	$\Delta\sigma^b_{n,50\%}$ MPa	$\Delta K^N_{1,50\%}$ MPa (mm)$^{0.5}$	$\Delta\overline{W}_{50\%}$ MJ/m^3
											Mean values at $N = 5 \times 10^6$ cycles		
St-42	Balasubramanian and Guha, 1999a	C-LC	ASTM 517F	T	8	790	1	2.000	0.875	0.687	101	197	0.089
St-43	Balasubramanian and Guha, 1999a	C-LC	ASTM 517F	T	8	790	1	1.600	0.925	0.821	85	197	0.090
St-44	Balasubramanian and Guha, 1999a	C-LC	ASTM 517F	T	8	790	1	1.200	0.875	0.935	69	183	0.078
St-45	Balasubramanian and Guha, 1998, 1999b	C-LC	ASTM 517F	T	8	790	1	2.000	0.900	0.699	88	174	0.070
St-46	Balasubramanian and Guha, 1998, 1999b	C-LC	ASTM 517F	T	8	790	1	1.200	0.660	0.767	68	147	0.050
St-47	Balasubramanian and Guha, 1998, 1999b	C-LC	ASTM 517F	T	8	790	1	2.000	1.200	0.843	78	186	0.080
St-48	Balasubramanian and Guha, 1998, 1999b	C-LC	ASTM 517F	T	8	790	1	1.200	0.880	0.939	58	155	0.055
St-49	Balasubramanian and Guha, 1999c	C-LC	ASTM 517F	T	8	790	1	2.000	0.900	0.699	108	214	0.106
St-50	Balasubramanian and Guha, 1999c	C-LC	ASTM 517F	T	8	790	1	1.200	0.660	0.767	83	179	0.074
St-51	Balasubramanian and Guha, 1999c	C-LC	ASTM 517F	T	8	790	1	1.600	0.910	0.812	96	221	0.112
St-52	Balasubramanian and Guha, 1999c	C-LC	ASTM 517F	T	8	790	1	2.000	1.200	0.843	89	212	0.104
St-53	Balasubramanian and Guha, 1999c	C-LC	ASTM 517F	T	8	790	1	1.200	0.880	0.939	70	187	0.080
St-54	Guha, 1995	C-LC	C-Mn	T	12.5	480	1	–	–	–	–	256	0.151
St-55	Ouchida and Nishioka,1966	C-LC	SM 41	T	32	450	1	1.125	0.438	0.613	48	168	0.065
St-56	Ouchida and Nishioka, 1966	C-LC	SM 41	T	16	450	1	1.125	0.438	0.613	73	178	0.073
St-57	Ouchida and Nishioka, 1966	C-LC	SM 41	T	32	450	1	0.625	0.375	0.644	61	222	0.114
St-58	Ouchida and Nishioka, 1966	C-LC	SM 41	T	16	450	1	0.625	0.375	0.644	79	204	0.096
St-59	MacFarlane and Harrison,1995	C-LC	BS 15	T	12.5	420	1	1.250	1.000	1.015	44	156	0.056
St-60	MacFarlane and Harrison,1995	C-LC	BS 15	T	12.5	420	1	1.250	1.000	0.746	54	144	0.047

St-61	Yamaguchi et al., 1966	C-LC	SM 41	T	10	450	1	2.000	1.000	0.746	94	223	0.115
St-62	Yamaguchi et al., 1966	C-LC	HT 60	T	10	600	1	2.000	1.000	0.746	92	216	0.108
St-63	Singh et al., 2003a	C-LC	AISI 304 L	T	6	622	1	1.333	0.333	0.495	145	175	0.071
St-64	Singh et al., 2003a	C-LC	AISI 304 L	T	6	622	1	1.333	0.500	0.619	131	198	0.091
St-65	Singh et al., 2003a	C-LC	AISI 304 L	T	6	622	1	1.333	0.667	0.734	112	202	0.094
St-66	Singh et al., 2003a	C-LC	AISI 304 L	T	6	622	1	1.333	1.000	0.974	87	208	0.100
St-67	Singh et al., 2003b	C-LC	AISI 304 L	T	6	622	1	1.333	0.667	0.734	96	173	0.069
St-68	Infante et al., 2003	C-LC	Duplex 2205	T	10	797	1	1.600	1.000	0.866	50	138	0.044

σ_u – ultimate tensile strength.

Type of joint: C-LC – cruciform joint with load-carrying fillet weld.

[a] For all series k_1 has been determined by means Equations (B.1).

[b] For ASTM 517F the mean value at 5×10^6 cycles was calculated by imposing a slope equal to 3.0.

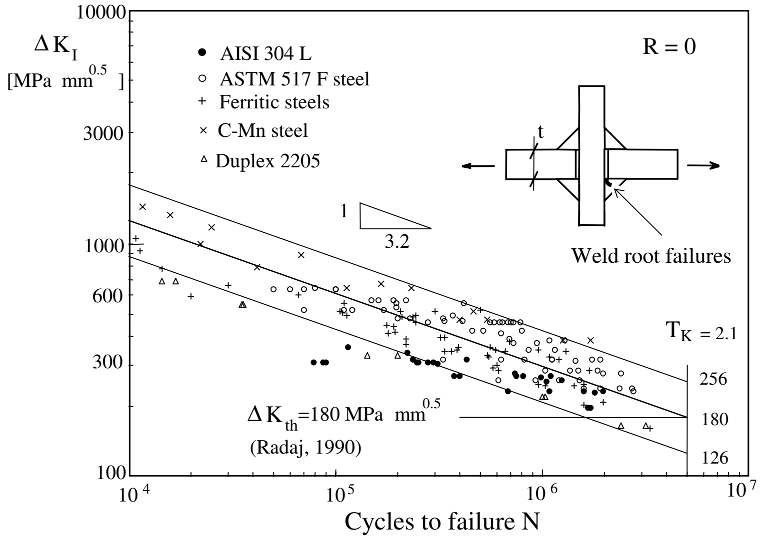

Figure 4. Fatigue strength of steel welded joints with $2\alpha = 0$ as a function of Mode I Stress Intensity Factor. Scatter band defined by mean values ± 2 standard deviations.

excluding from the statistical analysis the austenitic steels AISI 304L and Duplex 2205. It should be noted that the fatigue behaviour of the AISI 304L steel is substantially different in the medium fatigue range, whereas in the high cycle fatigue range its fatigue strength turns out to be comparable to that of the other steels. As far as steel Duplex 2205 is concerned, fatigue data are below or close to the lower limit of the band, despite the fact that the ultimate tensile strength of the parent material was equal to 797 MPa. Conversely, welded joints made of C–Mn steel show a systematically greater strength than the mean curve. These fatigue data are taken directly from a $\Delta K_\mathrm{I} - N$ plot reported by Guha (1995), where the total fatigue life was plotted against the parameter ΔK_I related to fatigue crack initiation life. The relevant mode I parameter at 5 million cycles is found to assume the maximum value (256 MPa(mm)$^{0.5}$, see series St-54 in Table 5). In order to use Frank and Fisher's equations in the presence of failures originated from the weld roots, it was necessary to simplify the weld bead geometry, by assuming a straight weld profile with $2\alpha = 135°$. This simplification was applied, in particular, to all welded joints analysed by Balasubramanian and Guha (1998, 1999a–c). A number of FE analyses showed that the influence of the weld bead shape on ΔK_I is weak when the fatigue crack initiates from the weld root.

Finally, it is interesting to learn that, for welded joints made of structural steels, Radaj (1990) reported different expressions for ΔK_th taken from the literature, from which $\Delta K_\mathrm{th} = 180$ MPa$\sqrt{\mathrm{mm}}$ (5.7 MPa m$^{1/2}$) represents the lower limit of scatter for $R = 0$. By considering the corresponding line drawn in Figure 4, only three points among 168 experimental data are below the recommended lower limit value. Two points are from Duplex 2205 steel.

3.1. Size effect

Figure 5 summarises in a double logarithmic diagram the mean values of fatigue strength at $N = 5 \times 10^6$ cycles for all series considered previously, by plotting the

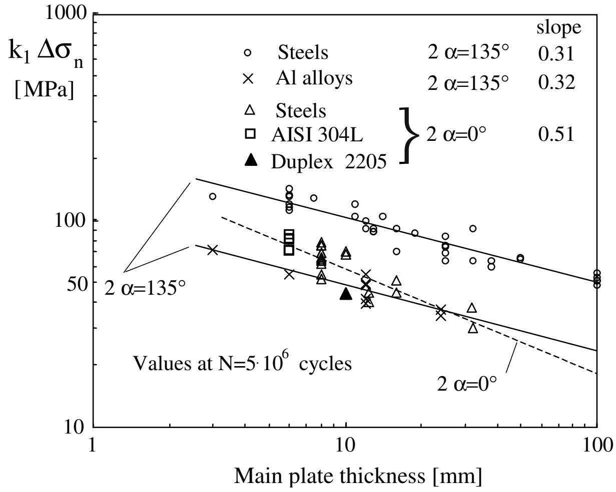

Figure 5. Fatigue strength of welded joints as a function of the main plate thickness ($R \approx 0$).

product $k_{1,j}\Delta\sigma_{n,j}$ against t_j, with t_j the main plate thickness of the j-series. A least square statistical analysis gave slopes equal to 0.31 and 0.32 for welded joints made of steel and aluminium alloys with ($2\alpha = 135°$), and equal to 0.51 for welded joints with failures from the roots ($2\alpha = 0°$). Since the theoretical values, according to the NSIF approach, should be $1 - \lambda_1 = 0.326$ and $1 - \lambda_1 = 0.5$, the agreement has to be considered very good. The former value confirms the prevailing role played by the nucleation and early propagation phases on the total fatigue life of the welded details analysed here. Dealing with scale effect, Macdonald and Haagensen (1999) emphasised the fact that assessment of recent research data had indicated an influence of thickness stronger than that suggested by Eurocode 3 (where the exponent is 0.25), so that, they wrote, in the latest HSE and API/ISO revision for offshore structures a higher penalty factor of 0.30 was imposed.

By using the scatter bands curves already shown reported in Figures 3 and 4 (which also include fatigue data obtained from AISI 304L and Duplex 2205) one can obtained some simplified rules to be applied at 5 million cycles by considering two different levels of probability of survival.

	P_s = 50%	P_s = 97.7%
Structural steel $2\alpha = 135°$:	$k_1\Delta\sigma_n = 210\,t^{-0.33}$	$k_1\Delta\sigma_n = 150\,t^{-0.33}$
Structural steel $2\alpha = 0°$:	$k_1\Delta\sigma_n = 180\,t^{-0.50}$	$k_1\Delta\sigma_n = 125\,t^{-0.50}$
Aluminium alloy $2\alpha = 135°$:	$k_1\Delta\sigma_n = 100\,t^{-0.33}$	$k_1\Delta\sigma_n = 70\,t^{-0.33}$

It is useful to note that:

- The exponents do not depend on the welded material, but only on the welded joint geometry.
- By keeping the main plate thickness t constant, the non-dimentional coefficient k_1 works like a stress concentration factor K_t; it makes it possible to establish the limit value of the nominal stress range under constant amplitude fatigue loading.

- From steel to aluminium there is a reduction factor equal to 2.1 when the V-notch angle is 135°. Exactly the same reduction was found to characterise high cycle fatigue strength of butt spliced bolted joints (Lazzarin et al., 1997).

4. Local-strain–energy based approach

It is well known that Equivalent Strain Energy Density (ESED) criterion (Glinka, 1985) can be used to determine the elastic–plastic stress and strain at the notch tip by imposing the constancy of the strain energy density with respect to the linear-elastic case. The criterion works well under plane strain conditions. For sharply V-shaped notches, the ESED criterion was recently extended from the notch tip to a finite size volume (area) surrounding the notch tip (Lazzarin and Zambardi, 2002). Under local yielding conditions, the constancy of the strain energy was used to evaluate plastic notch stress intensity factors (Lazzarin et al., 2001) simply by using the linear-elastic stress distribution.

Local strain energy density $\Delta\bar{W}$ averaged in a finite size volume surrounding weld toes and roots is a scalar quantity which can be given as a function of mode I-II NSIFs in plane problems (Lazzarin et al., 2003) and mode I-II-III NSIFs in three dimensional problems (Lazzarin et al., 2004). The evaluation of the local strain energy density needs precise information about the control volume size.

4.1. Value of the material parameter R_C for steel welded structures

From a theoretical point of view the material properties in the vicinity of the weld toes and the weld roots depend on a number of parameters as residual stresses and distortions, heterogeneous metallurgical micro-structures, weld thermal cycles, heat source characteristics, load histories and so on. To device a model capable of predicting R_C and fatigue life of welded components on the basis of all these parameters is really a task too complex. Thus, the spirit of this paper is to give a simplified method able to summarise the fatigue life of components only on the basis of geometrical information, treating all the other effects only in statistical terms, with reference to a well-defined group of welded materials and, for the time being, to arc welding processes. In the literature accurate analyses on the actual process zone in welded joints under static loading have been reported by Lin et al. (1999), who investigated the crack growth in a mis-matched single edge notched specimen under pure bending by means of a cohesive zone model. Under fatigue loading, the influence of plastic zone and plastic strain gradients were carefully analysed by Hadrboletz et al. (2001) in order to explain crack growth features from material defects.

Equation (9) makes it possible to estimate the R_C value as soon as ΔK_{1A}^N and $\Delta\sigma_A$ are known. At $N_A = 5 \times 10^6$ cycles and in the presence of a nominal load ratio R equal to zero, Figure 3 gives a mean value ΔK_{1A}^N equal to 211 MPa mm$^{0.326}$. For butt ground welds made of ferritic steels Atzori and Dattoma (1983) found a mean value $\Delta\sigma_A = 155$ MPa (at $N_A = 5 \times 10^6$ cycles, with $R = 0$). That value is in very good agreement with $\Delta\sigma_A = 153$ MPa recently obtained by Taylor et al. (2002) by testing butt ground welds fabricated of a low carbon steel. Then, by introducing the above mentioned value into Equation (9), one obtains for steel welded joints with failures from the weld toe $R_C = 0.28$ mm. The choice of 5 million cycles as a reference value is due

Table 6. Geometrical and fatigue strength properties of steel welded joints subjected to stress relieving. (nominal load ratio $R = 0$; radius $R_C = 0.28$ mm).

Series	Ref.	Welded joint geometry	Load	Material	σ_u MPa	t mm	L/t	$2h/t$	k_1	$\Delta\sigma_{n,50\%}$ MPa	$\Delta K^N_{1,50\%}$ MPa (mm)$^{0.326}$	$\Delta\bar{W}_{50\%}$ MJ/m^3
										Mean values at $N = 10^6$ cycles		
St-69	Gurney, 1991	C-NLC	T	BS 4360:50D	548[a]	13	0.769	1.231	1.141	138	364	0.174
St-70	Gurney, 1991	C-NLC	T	BS 4360:50	545[a]	25	0.120	0.400	0.787	169	379	0.189
St-71	Gurney, 1991	C-NLC	T	BS 4360:50	545[a]	25	0.520	0.800	1.038	141	418	0.229
St-72	Gurney, 1991	C-NLC	T	BS 4360:50	545[a]	25	8.800	1.200	1.359	110	427	0.240
St-73	Gurney, 1991	C-NLC	T	BS 4360:50D	531	50	0.060	0.200	0.641	172	395	0.205
St-74	Gurney, 1991	C-NLC	T	BS 4360:50D	531	50	4.400	0.600	1.41	93	467	0.287
St-75	Gurney, 1991	C-NLC	T	BS 4360:50D	509	100	0.030	0.100	0.551	149	369	0.179
St-76	Gurney, 1991	C-NLC	T	BS 4360:50D	509	100	0.130	0.160	0.647	141	409	0.220
St-77	Gurney, 1991	C-NLC	T	BS 4360:50D	509	100	2.000	0.300	1.239	80	445	0.260

σ_u – ultimate tensile strength.
Type of load: T – tension load.
Type of joint: C-NLC – cruciform joint with non-load-carrying fillet weld.
[a]Mean value from different plates with the same thickness.

Table 7. Geometrical and fatigue strength properties of aluminum welded joints under tension loads.(Nominal load ratio $R = 0.1$, radius $R_C = 0.12$ mm).

Series	Refs.	Geometry	Material	t mm	σ_u MPa	L/t	$2h/t$	k_1	k_2	$\Delta\sigma_{n,50\%}$ MPa	$\Delta K^N_{1,50\%}$ MPa mm$^{0.326}$	$\Delta K^N_{2,50\%}$ MPa (mm)$^{-0.302}$	$\Delta\bar{W}_{50\%}$ MJ/m^3
										Mean values at $N = 5 \times 10^6$ cycles			
AL-1	Maddox, 1995	C-NLC	6061-T6	3	329	1.000	3.000	1.22[a]	0.58[a]	59.3	103.2	24.8	0.072
AL-2	Maddox, 1995	C-NLC	6061-T6	6	301	1.000	2.333	1.21[a]	0.61[a]	45.3	97.8	16.1	0.064
AL-3	Maddox, 1995	C-NLC	6061-T6	12	317	1.000	1.667	1.19[a]	0.67[a]	40.5	108.6	12.8	0.079
AL-4	Maddox, 1995	C-NLC	6061-T6	24	313	1.000	1.708	1.19[a]	0.64[a]	29.1	97.7	7.1	0.064
AL-5	Maddox, 1995	C-NLC	6061-T6	24	313	0.250	0.583	0.91[a]	1.15[a]	40.9	105.0	18.0	0.074
AL-6	Maddox, 1995	C-NLC	6061-T6	12	317	0.500	1.167	1.10[a]	0.93[a]	38.0	94.1	16.6	0.060
AL-7	Meneghetti, 1998	T-NLC	5083-H3	12	330	0.833	1.333	0.93	1.22	43.1	89.7	24.8	0.054
AL-8	Ribeiro et al. (1995)	T-NLC	6061-T651	12	≈ 300	1.000[b]	1.333	0.93	1.22	53.0	110.3	30.5	0.082
AL-9	Ribeiro et al. (1995)	C-LC	6061-T651	12	≈ 300	1.000[b]	1.333	1.73	0.50	28.0	108.8	6.6	0.080
AL-10	Jacoby, 1961	C-LC	Al Zn Mg 1	12	384	1.000	1.060	2.07	0.72	26.3	122.5	8.9	0.101
											MPa mm$^{0.5}$	MPa mm$^{0.5}$	MJ/m^3
AL-11	Person, 1971	SL	5052-H32	4.8	210	–	2.000	0.75	1.19	15.1	24.9	39.5	0.073
AL-12	Person, 1971	SL	5083-H113	9.5	358	–	2.000	0.75	1.19	13.7	31.8	50.4	0.119
AL-13	Person, 1971	SL	7039-T61	9.5	402	–	2.000	0.75	1.19	13.3	30.7	48.7	0.111

Type of joint: C-NLC – cruciform joint with non-load carrying fillet weld; C-LC cruciform joint with load-carrying fillet weld; T-NLC – T-joint with non-load carrying fillet weld; SL – single lap joint.

[a] k_1 and k_2 have been determined by Equations (A.1) and (A.2). In the remaining cases, k_1 and k_2 have been determined by "ad hoc" FE analyses.

[b] Estimated from a figure of the original paper.

mainly to the fact that, according to Eurocode 3, nominal stress ranges corresponding to 5 million cycles can be considered as fatigue limits under constant amplitude load histories. It is worth noting that the simplified hypothesis of a semicircular core of radius R_C led to the assessment of a fatigue scatter band that exactly agreed with that of Haibach's normalised S–N band (see Haibach, 1989; Lazzarin et al., 2003).

In the case $2\alpha = 0$ and fatigue crack initiation at the weld root Equation (9) gives $R_C = 0.36$ mm, by neglecting the mode II contribution and using $e_1 = 0.133$, Equation (7), $\Delta K_{1A}^{N} = 180$ MPa mm$^{0.5}$, Figure (4), and, once again, $\Delta\sigma_A = 155$ MPa. There is a small difference with respect to the value previously determined, $R_C = 0.28$ mm. This fact is probably due to two concurrent events: welded material conditions are different at the weld root with respect to the weld toe and, more important, the group of welded steels considered in Figure 4 does not coincide with the previous one. However, in the safe direction, the proposal formulated here is to use $R_C = 0.28$ mm also for the welded joints with failures from the weld roots. A small decrease for R_C results in a small increase for the expected sensitivity to sharp V-notches.

More than 25 years ago Lawrence et al. (1978) proposed a model where total fatigue life was given as a sum of crack initiation life and crack propagation life. To quantify the former phase by using a local stress-life or strain-life approach, they suggested to average the stress amplitude at the weld toe at a given depth d. The same depth value d was afterwards used as initial crack length in the integration of the Paris law. It is surprising to note that the value $d = 0.25$ mm suggested by Lawrence et al. (1978) is very close to the values for R_C obtained here.

Finally, it is important to repeat that the obtained value for R_C has to be considered statistically valid only for arc welding technologies. Fatigue data from welded joints obtained by using high energy sources (the laser beam welding, for example) are not analysed here and are expected to give different value of R_C.

4.2. Value of the material parameter R_C for aluminium welded structures

With reference to aluminium welded structures, Figure 6 presents a number of fatigue data obtained from butt ground weld joints under a nominal load ratio $R = 0$. Details on material properties and geometrical parameters are reported in Table 8 where $\Delta\sigma_n$ ranges from 86 MPa to 107 MPa at 5×10^6 cycles, being 96 MPa the mean value. On the other hand, Figure 3 gave for aluminium welded joints a mean value for ΔK_{1A}^{N} equal to 99 MPa mm$^{0.326}$. By using such values into Equation (9) one obtains for aluminium welded joints a reference value $R_C =$ 0.12 mm. Then, by comparing steel and aluminium welded joints, the relevant R_C values are in the ratio 2.3. Radaj and Sonsino (1998) suggested a "microstructural support length" ρ^* equal to 0.4 mm for ferritic welded materials, and two different values for the aluminium alloy AlMg4.5Mn: $\rho^* = 0.14$ mm for the parent material and $\rho^* = 0.24$ mm for the welded material, being 0.17 mm the mean value. It is interesting to note that the ratio between the mean values of ρ^* is again 2.3.

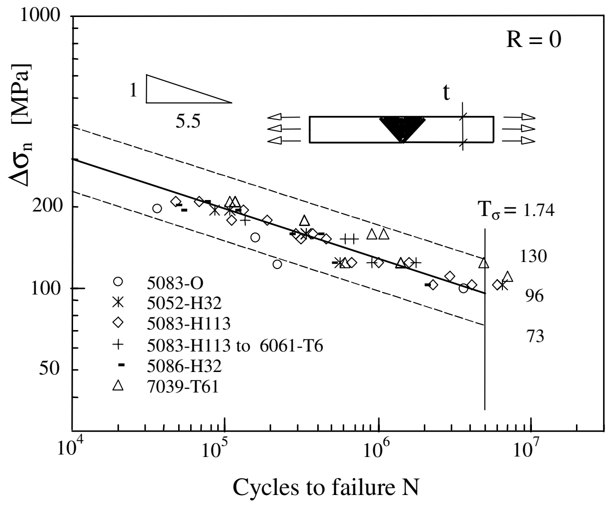

Figure 6. Fatigue strength of butt ground aluminium welded joints. Scatter band defined by mean values ±2 standard deviations.

Table 8. Static and fatigue properties of butt ground welded joints made of aluminum alloy. (Traction loads with a nominal load ratio $R = 0$).

Series	Refs	Material	t mm	σ_u MPa	$\Delta\sigma_{n,50\%}$ MPa $N = 5 \times 10^6$
AL-14	Ohno, 1985	5083-O	4	300	86
AL-15	Person, 1971	5052-H32	4.8	210	92
AL-16	Person, 1971	5083-H113	9.5	358	100
AL-17	Person, 1971	5083-H113:6061-T6	9.5	307–358	100
AL-18	Person, 1971	5086-H32	9.5	327	107
AL-19	Person, 1971	7039-T61	9.5	402	102

5. Fatigue strength in terms of strain energy in a finite size volume

By using more than 300 fatigue data related to the series reported in Tables 2 and 3, an energy based scatter band for steel welded joints was proposed by Lazzarin et al. (2003). Main plate thickness ranged from 6 mm to 100 mm whereas the V-notch angle ranged from 110° to 150°. All failures originated from the weld toe.

That band is shown in Figure 7 together with the new data already reported in Figure 3 ($2\alpha = 135°$) and Figure 4 ($2\alpha = 0$), independently from the fatigue crack initiation point. It is evident that the previous scatter band can be satisfactorily applied also to the new data, the only exceptions being austenitic steel AISI 304 L (for which the agreement is good only in the high cycle fatigue regime) and, partially, Duplex 2205 steel.

Due to the use of energy, not only the variability of $\Delta\bar{W}$ increases with respect to stress-based curves (from about 4.0 MJ/m^3 at 10^4 cycle to about 0.1 MJ/m^3 at 2×10^6 cycles, but also the scatter increases. However, as soon as one reconverts the $T_{\Delta\bar{W}}$

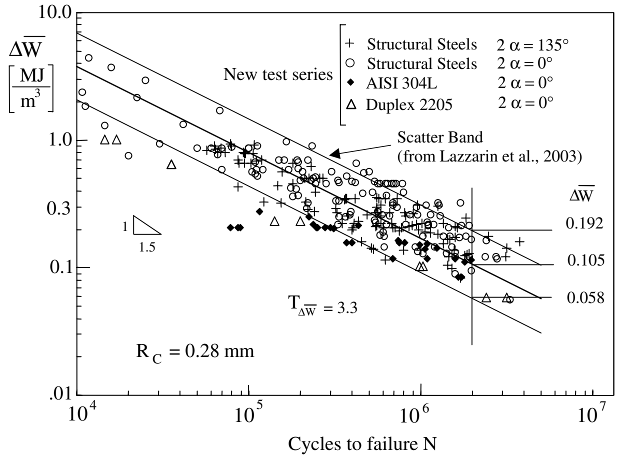

Figure 7. Strain energy-based scatter band summarising fatigue strength data of steel welded joints subjected to tension and bending loads; main plate thickness ranging from 3 to 100 mm, weld flank angle from 0° to 135°.

value (3.3) into the more usual T_σ value, referred to a 10–90% stress-based band, the result would be $T_\sigma = \sqrt{3.3}/1.21 = 1.50$. This value matches exactly the T_σ value of the Haibach 10–90% Normalised S–N Scatter Band for steel welded joints (Haibach, 1989; see also Radaj and Sonsino, 1998, p. 35).

Kept constant the nominal load ratio ($R = 0$), structural steels and welding process, the influence of residual stresses is shown in Figure 8, where fatigue data obtained by Gurney from stress relieved joints are plotted together with those obtained by the same Author by testing "as-welded" joints (Gurney, 1991). In the absence of any residual stress, the fatigue curve exhibits a knee in correspondence of about 10^6 cycles to failure, over which the fatigue strength of stress relieved specimens remains practically constant (the mean value being about equal to 0.14 MJ/m^3). Geometrical parameters of the stress relieved series as well as their fatigue strength data referred to one million cycles are summarised in Table 6.

The results related to aluminium alloy joints are shown in Figure 9, where the mean value of the strain energy density $\Delta\bar{W}$ is plotted as a function of cycles to failure. The new scatter band is characterised by a $T_{\Delta\bar{W}}$ index equal to 3.2, almost coincident with the value reported in Figure 7 for steel welded joints. A limited number of data related to single lap joints (where mode II contribution prevailed on mode I contribution) are seen to belong to the same scatter band. Finally, one should note that, by using $R_C = 0.28$ mm for steel welded joints and $R_C = 0.12$ mm for aluminium welded joints, the mean values of $\Delta\bar{W}$ at 2×10^6 cycles are very close.

Just by considering linear elastic behaviour and ideally sharp notches under static loads, Gómez and Elices (2003) were able to show that a single non-dimensional curve fits well experimental data from V-notched specimens of steel, aluminium, PMMA and PVC. Their curve plotted, as a function of the notch angle, the non-dimensional parameter $K_{IC}^{*,V}$, which combined together values of NSIF, fracture toughness K_{IC} and a characteristic length of the material L_{ch}. This length depends on K_{IC} and the ultimate tensile strength σ_u according to the expression $L_{ch} = (K_{IC}/\sigma_u)^2$. Under static conditions L_{ch} played the same role as R_C.

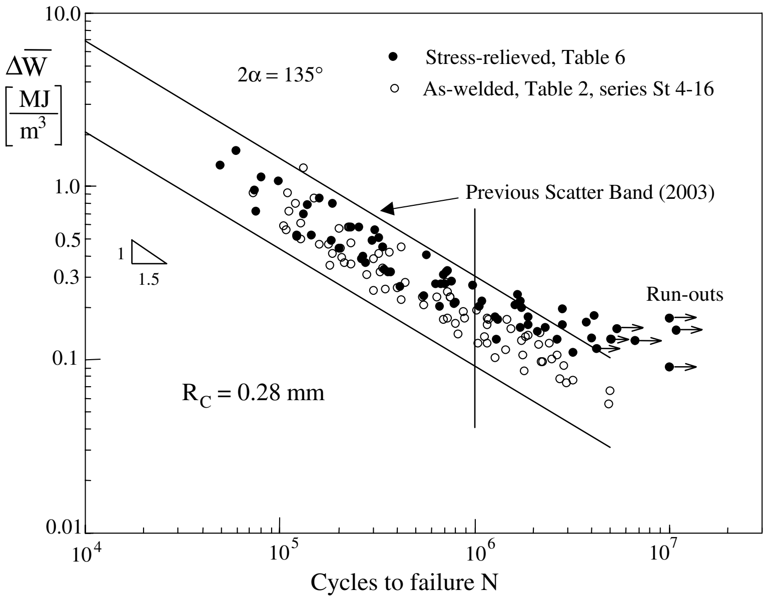

Figure 8. Fatigue strength of as-welded and stress-relieved welded joints ($R = 0$). Original stress-based data from Gurney (1991).

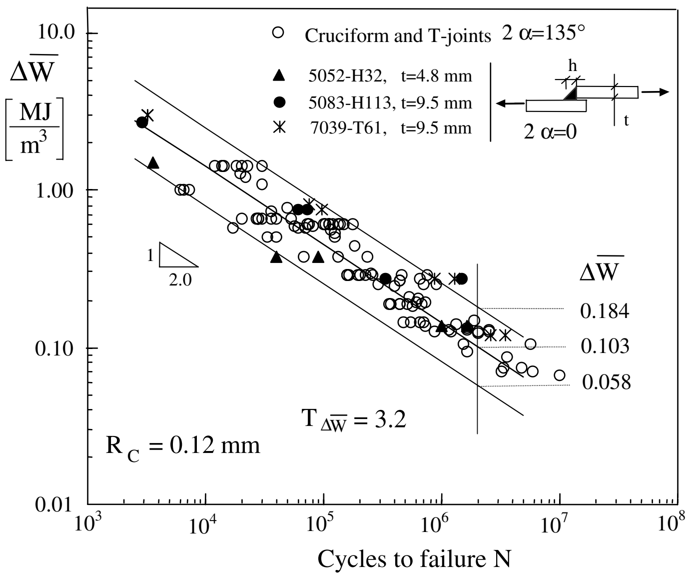

Figure 9. Strain energy-based scatter band summarising fatigue strength data of aluminium alloy welded joints subjected to tension and bending loads.

Finally, Figure 10 plots experimental data for steel and aluminium welded joints, with a common value of $\Delta\overline{W}$ at 2×10^6 cycles. Since slopes for steel and aluminium are different, the scatter band is reported only from 0.5×10^6 to 5×10^6 cycles to failure.

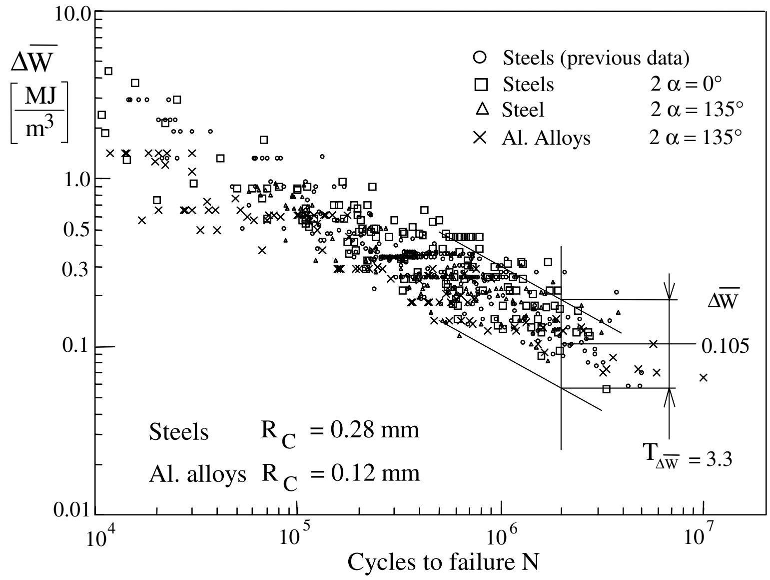

Figure 10. Strain energy-based scatter band summarising about 650 fatigue data of welded joints made of steel or aluminium alloy subjected to tension and bending loads (the main plate thickness ranging from 3 to 100 mm, the weld flank angle from 0° to 150°).

6. Conclusions

Consider a notch component with a certain notch root. Decreasing the notch root ρ, the theoretical stress concentration factor K_t increases and the fatigue limit decreases. Below a given critical value for ρ^*, the fatigue limit is no longer controlled by K_t and the notch behaves like a crack of equal depth. In the welded joints the conventional welding procedures result in small value of the weld toe and the weld root radius. In this paper this value is considered insignificant and fatigue life assessments are performed on the basis of the NSIFs, which are determined by modelling the highly stressed regions as sharp, zero radius, V-notches.

Fatigue damage is generally described as the nucleation and growth of cracks to final failure, although the differentiation of two stages is qualitatively distinguishable but quantitatively ambiguous. Therefore, the paper operates a second strong simplification. Since most of the fatigue life is micro-crack propagation within the region of the virtual singularity due to the notch, it is not necessary to distinguish initiation and micro-crack propagation and the total fatigue life is directly correlated to NSIF. This assumption has been verified by proposing some NSIF-based scatter bands related to steel and aluminium welded joints subjected to a nominal load ratio close to zero. More precisely, the bands are related to:

- steel welded joints with failures originated from the weld toe, in the presence of a V-notch angle 2α about equal to 135°. Under such conditions, only mode I NSIF was significant, since stress distributions ascribable to the sliding mode were non-singular. At 5×10^6 cycles to failure, the mean values of mode I NSIF turned out to be $\Delta K_{1A}^{N}=211$ MPa (mm)$^{0.326}$; the scatter index of the 2.3–97.7% band was 1.8. It was noted that the scatter index would be 1.5 for the 10–90% band, exactly as

happens in Haibach's normalised S–N Band. The synthesis involved welded joints with a main plate thickness ranging from 3 mm to 100 mm.
- aluminium welded joints under the same load and geometrical conditions. At 5×10^6 cycles to failure, the mean values of ΔK_{1A}^{N} was 99 MPa (mm)$^{0.326}$.
- steel welded joints with failures from the weld roots. Statistical analysis gave ΔK_{1A}^{N}= 180 MPa (mm)$^{0.5}$.

Due to their nature, NSIFs fully include the scale effect. The statistical re-analysis of fatigue showed that the scale effect was ruled by an exponent about equal to 0.3 for aluminium and steel welded joints with $2\alpha = 135°$, while a value equal to 0.5 is realistic for the welded joints with failure from the weld root. This means that the exponent 0.25 suggested by Eurocode 3 is non-conservative when applied to the geometries considered here.

Units for NSIFs vary according to the V-notch angle. In order to collect fatigue data obtained from joints with different values of 2α, as well as cases of failures from weld root and weld toe, a third simplifying assumption was made in the paper. The parameter used is a simple scalar quantity, the strain energy range included in a control volume being represented by a semicircular sector of radius R_C. The strain energy density was evaluated under the plane strain hypothesis, assuming for the material a linear elastic law. Analyses showed that:

- as happens for the El Haddad material parameter a_0, the evaluation of R_C needs the determination of an NSIF-based curve and the high cycle fatigue strength of butt ground welded joints.
- the radius R_C was 0.28 mm for steel welded joints and 0.12 mm for aluminium welded joints.
- Thanks to different values of the Young modulus and the radius R_C, the mean values of the strain energy density at 2×10^6 cycles turned out to be practically the same for steel and for aluminium welded joints (0.105 MJ/m^3 against 0.103 MJ/m^3). Both values are valid under a nominal load ratio about equal to zero, with reference to the welded materials detailed in the present paper.
- Quite different was the behaviour of some welded joints in AISI 304L. They showed a mean value of the strain energy range in agreement with that of the band but only at a high number of cycles. In the low-medium life regime their energy-based curve was noticeably lower. This holds true also for a series of welded joints of reduced thickness (3 mm) made of a high strength steel.

Appendix A

Expressions for k_1 and k_2 have already been reported for transverse non-load carrying fillet welded joints subjected to tension (Lazzarin and Tovo, 1998) or bending loads (Atzori et al., 1999b). It is useful to report here such expressions since most welded details considered herein just refer to such type of joints.

Tension:

$$k_1 = 1.212 + 0.495e^{-0.985(2h/t)} - 1.259e^{-1.120(2h/t)-0.485(L/t)}, \tag{A.1}$$

$$k_2 = 0.508 - 0.797e^{-1.959(2h/t)} + 2.723e^{-1.126(2h/t)-0.769(L/t)}. \tag{A.2}$$

Bending:

$$k_1 = 0.900 + 0.326e^{-5.289(2h/t)} - 0.474e^{-3.064(2h/t)-1.420(L/t)}, \tag{A.3}$$

$$k_2 = 0.818 - 1.760e^{-5.356(2h/t)} + 1.851e^{-2.982(2h/t)-1.026(L/t)}. \tag{A.4}$$

According to symbols shown in Figure 2, h is the height of the weld bead and L, the transverse plate thickness. Estimates based on Equations (A.1) and (A.2) are accurate when $0 \leq L/t \leq 3.0$ and $0.25 \leq 2h/t \leq 2.5$. Limits of Equations (A.3) and (A.4) are $0.2 \leq L/t \leq 5.0$ and $0.25 \leq 2h/t \leq 2.5$. Out of these geometrical conditions, a finite element analysis should be carried out.

Appendix B

The SIF of load-carrying cruciform joints with failure from the weld root can be calculated by means of Frank and Fischer's equations (1979). These equations take into account the variation of the main geometrical parameters: plate thickness, dimensions of the fillet and the lack of penetration zone. The weld profile was modelled like a sharp V-notch with an opening angle of 135°. Furthermore, the transverse plate thickness was equal to the main plate thickness. Mode I NSIF is

$$K_I = \frac{\sigma_n \left(A_1 + A_2 \frac{a}{w}\right) \sqrt{\pi a \sec \frac{\pi a}{2w}}}{1 + \frac{2h}{t}}, \tag{B.1}$$

where symbols a, h, and t are as shown in Figure 2 and $w = h + t/2$. The value of the nominal stress σ_n has to be referred, as usual, to the longitudinal plates of thickness t. Parameters A_1 and A_2 depend on the h/t ratio and are given by the following polynomials (Frank and Fisher, 1979)

$$A_1 = 0.528 + 3.287\frac{h}{t} - 4.361\left(\frac{h}{t}\right)^2 + 3.696\left(\frac{h}{t}\right)^3 - 1.875\left(\frac{h}{t}\right)^4 + 0.415\left(\frac{h}{t}\right)^5, \tag{B.2}$$

$$A_2 = 0.218 + 2.717\frac{h}{t} - 10.171\left(\frac{h}{t}\right)^2 + 13.122\left(\frac{h}{t}\right)^3 - 7.755\left(\frac{h}{t}\right)^4 + 1.783\left(\frac{h}{t}\right)^5. \tag{B.3}$$

As recently underlined by Singh et al. (2003a), British Standard BS 7910 (2001) gives stress intensity factor values according to Equations (B.1–B.3).

Moreover the effect of the transverse plate thickness was analysed by means of three FE models where L/t was 0.5, 1.0, and 2.0, respectively, whereas $2h/t$ and a/t were kept constant ($2h/t = 4/3$ and $a/t = 1/3$). Results for k_1 were 0.488, 0.517, and 0.522, respectively. The value of 0.517 is in good agreement with the value of 0.495 provided by Equation (B.1). All FE analyses confirmed that the contribution due to mode II is negligible with respect to that of mode I.

Appendix C

A number of FE analyses have considered transverse load-carrying fillet welded joints with $2\alpha = 135^\circ$ at the weld toe, in the presence of main plate and transverse plates of equal thickness. Non-dimensional coefficients for opening and sliding modes are given by Equations (C.1) and (C.2), to be used when fatigue failure initiates from the weld toes and the ratio between the zone of lack of penetration and the main thickness equals unity

$$k_1 = 1.247 + 6.492e^{-2h/0.513t} \tag{C.1}$$

$$|k_2| = \left|-0.548 + 2.669e^{-2h/1.423t}\right| \tag{C.2}$$

Acknowledgements

The authors wish to thank the Italian Ministry of University and Scientific Research and the University of Padova for funding this research (project codes: PRIN 2004082252 and CPDA_035135).

References

Atzori, B. and Dattoma, V. (1983). A comparison of the fatigue behaviour of welded joints in steels and in aluminium alloys. IIW Doc XXXIII-1089-1983.

Atzori, B. (1985). Notch effect or Linear Elastic Fracture Mechanics in fatigue design. *Proceedings XIII Congress of Italian Society for Strain Analysis* Bergamo, Italy, AIAS ed.

Atzori, B., Lazzarin, P. and Tovo, R. (1999a). From the local stress approach to fracture mechanics: a comprehensive evaluation of the fatigue strength of welded joints. *Fatigue and Fracture of Engineering Materials and Structures* **22**, 369–382.

Atzori, B., Lazzarin, P. and Tovo, R. (1999b). Stress field parameters to predict the fatigue strength of notched components. *Jounal of Strain Analysis* **34**, 437–453.

Atzori, B., Meneghetti, G. and Susmel, L. (2002). Estimation of the fatigue strength of light alloy welds by an equivalent notch stress analysis. *International Journal of Fatigue* **24**, 591–599.

Balasubramanian, V. and Guha, B. (1998). Influence of flux cored arc welded cruciform joint dimensions on fatigue life of ASTM 517 F grade steels. *Internation Journal of Pressure Vessels and Piping* **75**, 765–772.

Balasubramanian, V. and Guha, B. (1999a). Effect of welded size on fatigue crack growth behaviour of cruciform joints by strain energy density factor approach. *Theoretical and Applied Fracture Mechanics* **31**, 141–148.

Balasubramanian, V. and Guha, B. (1999b). Optimising the shielded metal arc welded cruciform joint dimensions of ASTM 517 F grade steels containing LOP defects. *International Journal of Pressure Vessels and Piping* **76**, 147–155.

Balasubramanian, V. and Guha, B. (1999c). Fatigue life prediction of shielded metal arc welded cruciform jonts containing LOP defects by a mathematical model. *International Journal of Pressure Vessels and Piping* **76**, 283–290.

Boukharouba, T., Tamine, T., Nui, L., Chehimi, C. and Pluvinage, G. (1995). The use of notch stress intensity factor as a fatigue crack initiation parameter. *Engineering Fracture Mechanics* **52**, 503–512.

British Standard Institution. Guidance on method for the acceptance of flaws in structures. PD 6493, BS 7910, Appendix J; 2001.

Dunn, M.L., Suwito, W. and Cunningham, S. (1997). Fracture initiation at sharp notches: Correlation using critical stress intensities, *International Journal of Solids and Structures* **34**, 3873–3883.

El Haddad, M.H., Topper, T.H. and Smith, K.N. (1979). Fatigue crack propagation of short cracks", *ASME, Journal of Engineering Materials and Technology* **101**, 42–45.

Engesvik, K. and Lassen, T. (1988). The effect of weld geometry on fatigue life. *Proceedings of the 3rd International OMAE Conference*, Houston, Texas, 440–446.

Frank, H. and Fisher, J.W. (1979). Fatigue strength of fillet welded cruciform joints, ASCE, *Journal of the Structural Division* **20**, 1727–1740.

Glinka, G. (1985). Energy density approach to calculation of inelastic strain-stress near notches and cracks. *Engineering Fracture Mechanics* **22**, 485–508.

Gómez, F.J. and Elices, M. (2003). A fracture criterion for sharp V-notched samples. *Internation Journal of Fracture* **123**, 163–175.

Gómez, F.J. and Elices, M. (2004). A fracture criterion for blunted V-notched samples. *Internation Journal of Fracture* **127**, 239–264.

Gross, R. and Mendelson, A. (1972). Plane elastostatic analysis of V-notched plates. *International Journal of Fracture Mechanics* **8**, 267–276.

Guha, B. (1995). A new fracture mechanics method to predict the fatigue life of welded cruciform joints. *Engineering Fracture Mechanics* **52**, 215–229.

Gurney, TR. (1991). *The Fatigue Strength of Transverse Fillet Welded Joints*. Abington Publishing, Cambridge.

Gurney, TR. (1997). *Fatigue of Thin Walled Joints Under Complex Loading*. Abington Publishing, Cambridge.

Gustafsson, M. (2002). Thickness effect in fatigue of welded extra high strength steel joints, In: Design and analysis welded high strength steel structures (Ed. J. Samuelsson), Fatigue, 205–224.

Hadrboletz, A. Weiss, B. and Khatibi, G. (2001). Fatigue and fracture properties of thin metallic foils. *Internation Journal of Fracture* **109**, 69–89.

Haibach, E. (1989). *Service Fatigue-Strength – Methods and data for structural analysis*. Dusseldorf, VDI, 1992.

Infante, V., Branco, M. and Martins, R. (2003). A fracture mechanic analysis on the fatigue behaviour of cruciform joints of duplex stainless steel, *Fatigue and Fracture of Engineering Materials and Structures* **26**, 791–810.

Jiang, Y. and Feng, M. (2004). Modeling of fatigue crack propagation. *Journal of Engineering Materials and Technology* **126**, 77–86.

Jacoby, G. (1961). Über das verhalten von schweissverbindungen aus aluminiumlegierungen bei schwingbeanspruchung. Dissertation, Technische Hochschule, Hannover.

Kihara, S. and Yoshii, A. (1991). A strength evaluation method of a sharply notched structure by a new parameter, "The Equivalent Stress Intensity Factor". *JSME International Journal* **34**, 70–75.

Kihl, D.P. and Sarkani, S. (1997). Thickness effects on the fatigue strength of welded steel cruciforms. *Internation Journal of Fatigue* **19**, S311–S316.

Kihl, D.P. and Sarkani, S. (1999). Mean stress effects in fatigue of welded steel joints. *Probabilistic Engineering Mechanics* **14**, 97–104.

Kloppel, K. and Weihermuller, H. (1959). Dauerfestigkeitsversuche mit schweissuerbindindungen stabarschlussen. *Stahlbau* **5**, 149–155. ESDU 75016.

Lassen, T. (1990). The effect of the welding process on the fatigue crack growth. *Welding Journal* **69**, Research Supplement, 75S–81S.

Lazzarin, P. and Tovo R. (1996). A unified approach to the evaluation of linear elastic fields in the neighbourhood of cracks and notches. *International Journal of Fracture* **78**, 3–19.

Lazzarin, P., Milani, V. and Quaresimin M. (1997). Scatter bands summarizing the fatigue properties of symmetric splice bolted joints in light alloy. *Internation Journal of Fatigue* **19**, 401–407.

Lazzarin, P. and Tovo, R. (1998). A notch intensity approach to the stress analysis of welds. *Fatigue and Fracture of Engineering Materials and Structure* **21**, 1089–1104.

Lazzarin, P. and Livieri, P. (2001). Notch stress intensity factors and fatigue strength of aluminium and steel welded joints. *International Journal of Fatigue* **23**, 225–232.

Lazzarin, P., Zambardi, R. and Livieri, P (2001). Plastic notch stress intensity factors for large V-shaped notches under mixed load conditions. *International Journal of Fracture* **107**, 361–377.

Lazzarin, P. and Zambardi, R. (2001). A finite-volume-energy based approach to predict the static and fatigue behaviour of components with sharp V-shaped notches. *International Journal of Fracture* **112**, 275–298.

Lazzarin, P. and Zambardi, R. (2002). The equivalent strain energy density approach reformulated and applied to sharp V-shaped notches under localised and generalised plasticity. *Fatigue and Fracture of Engineering Materials and Structure* **25**, 917–928.

Lazzarin, P., Lassen, T. and Livieri, P. (2003). A notch stress intensity approach applied to fatigue life predictions of welded joints with different local toe geometry, *Fatigue and Fracture of Engineering Materials and Structures* **26**, 49–58.

Lazzarin P., Sonsino, C.M. and Zambardi, R. (2004). A notch stress intensity approach to predict the fatigue behaviour of T butt welds between tube and flange when subjected to in–phase bending and torsion loading, *Fatigue and Fracture of Engineeering Materials and Structures* **27**, 127–141.

Lawrence, F.V., Mattos, R.J., Higashida, Y. and Burk, J.D. (1978). Estimating the fatigue crack initiation life at welds. In: Fatigue Testing of Weldments, ASTM STP 648. ASTM, Philadelphia, 134–158.

Lin, G., Meng, X.G., Cornec, A. and Schwalbe, K.H. (1999). The effect of strength mis-match on mechanical performance of weld joints, *International Journal of Fracture* **96**, 37–54.

Macdonald, K.A. and Haagensen, P.J. (1999). Fatigue design of welded aluminium rectangular hollow section joints. *Engineering Failure Analysis* **6**, 113–130.

Macfarlane, D.S. and Harrison, J.D. (1995). Some fatigue tests on load-carrying tranverse fillet welds. *British Welding Journal* **12**, 613–623. ESDU 75016.

Maddox. S.J. (1987). *The Effect of Plate Thickness on the Fatigue Strength of Fillet Welded Joints*. Abington Publishing, Abington, Cambridge.

Maddox, S.J. (1995). Scale effect in fatigue of fillet welded aluminium alloys. *Proceedings of the Sixth International Conference on Aluminium Weldments*, Cleveland, Ohio, 77–93.

Meneghetti, G. (1998). PhD Thesis, University of Padova.

Ouchida, H. and Nishioka, A. (1966). A study of fatigue strength of fillet welded joints. *Schweisstechnic* **16**, 150-157. (English translation: International Institute of Welding, Document XIII Series, N° 338, 1964). ESDU 75016.

Ohno, H. (1985). Improvement of fatigue strength of alluminium alloy welded joints by toe peening. Welding Institute of Japan Collected Paper Vol. 3. ESDU 91039.

Person, N.L. (1971). Fatigue of aluminium alloy welded joints, *Welding Research Supplement* **50**, 77s–87s.

Radaj, D. (1990). *Design and Analysis of Fatigue Resistant Welded Structures*, Abington Publishing, Cambridge.

Radaj, D. and Sonsino, C.M. (1998). *Fatigue Assessment of Welded Joints by Local Approaches*, Abington Publishing, Cambridge.

Riberio, A.S., Gonçalves, J.P., Oliveria, F., Castro, P.T. and Fernandes, A.A. (1995). A compartive study on the fatigue behaviour of aluminium alloy welded and bonded Joints. *Proceeding of the Sixth International* Conference on Aluminium Weldments, Cleveland, Ohio, 65–76.

Ribeiro, A.S., Gonçalves, J.P., Oliveira, F., Castro, P.T., Fernandes, A.A. (1995). A comparative study on the fatigue behaviour of aluminium alloy welded and bounded Joints. Proc. Sixth Int. Conference on Aluminium Weldments, Cleveland, Ohio, 65–76.

Seweryn, A., Poskrobko, S. and Mróz, Z. (1997). Brittle fracture in plane elements with sharp notches under mixed-mode loading. *Journal of Engineering Mechanics* **123**, 535–543.

Sheppard, S.D. (1991). Field effects in fatigue crack initiation: long life fatigue strength', Trans. ASME, *J Mechanical Design* **113**, 188–194.

Singh, P.J., Achar, D.R.G., Guha, B. and Nordberg, H. (2003a). Fatigue life prediction of gas tungsten arc welded AISI 304L cruciform joints different LOP sizes. *International Journal of Fatigue* **25**, 1–7.

Singh, P.J., Guha, B., Achar, D.R.G. and Nordberg, H. (2003b). Fatigue life prediction improvement of AISI 304L cruciform welded joints by cryogenic treatment. *Engineering Failure Analysis* **10**, 1–12.

Sonsino, C.M. (1995). Multiaxial fatigue of welded joints under in-phase and out-of-phase local strains and stresses. *International Journal of Fatigue* **17**, 55–70.

Taylor, D. (1999). Geometrical effects in fatigue: a unifying theoretical model, *International Journal of Fatigue* **21**, 413–420.

Taylor, D., Barrett, N. and Lucano, G. (2002). Some new recent methods for predicting fatigue in welded joints. *International Journal of Fatigue* **24**, 509–518.

Verreman, Y. and Nie, B. (1996). Early development of fatigue cracking at manual fillet welds, *Fatigue and Fracture of Engineering Materials and Structures* **19**, 669–681.

Williams, M.L. (1952). Stress singularities resulting from various boundary conditions in angular corners of plates in extension. *Journal of Applied Mechanics* **19**, 526–528.

Yakubovskii, V.V. and Valteris, I.I. (1989). Geometrical parameters of butt and fillet welds and their influence on the welded joints fatigue life. *International Institute of Welding*, Document XIII-1326–89.

Yamaguchi, I., Terada, Y. and Nitta, A. (1966). Fatigue strength of steels for whip structures. International Institute of Welding, Document XIII Series, No. 425. ESDU 75016.